

Anisotropic Motion of Cholesterol in Oriented DPPC Bilayers Studied by Quasielastic Neutron Scattering: The Liquid-Ordered Phase

Christine Gliss,^{*} Oliver Randel,[#] Helene Casalta,[#] Erich Sackmann,[§] Reiner Zorn,[¶] and Thomas Bayerl^{*}

^{*}Institut für Experimentelle Physik, V, Universität Würzburg, 97074 Würzburg, Germany; [#]Institute Max von Laue–Paul Langevin, 38042 Grenoble Cedex 9, France; [§]Institut für Biophysik, Technische Universität München, D-85748 Garching, Germany; and [¶]Institut für Festkörperphysik, Forschungszentrum Jülich, 52424 Jülich, Germany

ABSTRACT Quasielastic neutron scattering (QENS) at two energy resolutions (1 and 14 μeV) was employed to study high-frequency cholesterol motion in the liquid ordered phase (lo-phase) of oriented multilayers of dipalmitoylphosphatidylcholine at three temperatures: $T = 20^\circ\text{C}$, $T = 36^\circ\text{C}$, and $T = 50^\circ\text{C}$. We studied two orientations of the bilayer stack with respect to the incident neutron beam. This and the two energy resolutions for each orientation allowed us to determine the cholesterol dynamics parallel to the normal of the membrane stack and in the plane of the membrane separately at two different time scales in the GHz range. We find a surprisingly high, model-independent motional anisotropy of cholesterol within the bilayer. The data analysis using explicit models of molecular motion suggests a superposition of two motions of cholesterol: an out-of-plane diffusion of the molecule parallel to the bilayer normal combined with a locally confined motion within the bilayer plane. The rather high amplitude of the out-of-plane diffusion observed at higher temperatures ($T \geq 36^\circ\text{C}$) strongly suggests that cholesterol can move between the opposite leaflets of the bilayer while it remains predominantly confined within its host monolayer at lower temperatures ($T = 20^\circ\text{C}$). The locally confined in-plane cholesterol motion is dominated by discrete, large-angle rotational jumps of the steroid body rather than a quasicontinuous rotational diffusion by small angle jumps. We observe a significant increase of the rotational jump rate between $T = 20^\circ\text{C}$ and $T = 36^\circ\text{C}$, whereas a further temperature increase to $T = 50^\circ\text{C}$ leaves this rate essentially unchanged.

INTRODUCTION

The effect of cholesterol on the physical properties of phospholipid bilayers has been studied extensively by a wide variety of methods, particularly for binary phospholipid/cholesterol mixtures (recently reviewed in McMullen and McElhaney, 1996). Because cholesterol may account for up to 50% of the total lipid in biological membranes, considerable experimental (Vist and Davis, 1990; Finegold, 1993; Ipsen et al., 1990; Almeida et al., 1992; Smaby et al., 1994) and theoretical (Ipsen et al., 1987; Gabdoulline et al., 1996; Tobias et al., 1997; Tu et al., 1998; Ipsen et al., 1989) research has been focused on the cholesterol-rich, so-called liquid-ordered phase (lo-phase) of binary lipid/cholesterol mixtures. This phase was found to exhibit fluid-like membrane properties and high molecular order of the lipid chains. The studies suggest that a comprehensive understanding of the properties of the lo-phase cannot be reached without considering its molecular dynamics. Although lipid dynamics has been studied up to the terahertz frequency range (König et al., 1992; König and Sackmann, 1996), information about the cholesterol dynamics in this frequency range is scarce. In particular, there is a lack of information on the motional anisotropy of cholesterol in a phospholipid bilayer with respect to directions parallel and

perpendicular to the bilayer normal. There are some results for motions within the plane of the bilayer: NMR relaxation studies have revealed details of the rotational motion of this steroid in the bilayer plane (Brown, 1990; Bonmatin et al., 1990). NMR and IR studies showed the conformational order and the chain dynamics of lipid/cholesterol systems (Davies et al., 1990; Siminovitch et al., 1987, 1988). The dynamics along the membrane normal is of particular importance for our understanding of the liquid-ordered phase. It has been suggested that cholesterol may bind via hydrogen bonds to moieties in the choline headgroup. This would drastically restrict its motional freedom in direction along the membrane normal. Furthermore, a number of recent experimental results have questioned the alleged homogeneity of the liquid-ordered phase with respect to changes in cholesterol concentration and temperature (Bayerl and Sackmann, 1993; Reinl et al., 1992; Huang et al., 1993). So far, no evidence from the dynamics of cholesterol in bilayers has been provided that would allow researchers to decide whether this phase is homogeneous or heterogeneous. In previous studies we have employed quasielastic neutron scattering (QENS) to resolve the high-frequency dipalmitoylphosphatidylcholine (DPPC) dynamics in thin bilayers (König et al., 1992; König and Sackmann, 1996).

Here we report the first QENS study on the dynamics of cholesterol in fully hydrated oriented multilayers of binary DPPC/cholesterol mixtures in the concentration range corresponding to the liquid-ordered phase (40 mol% cholesterol). By measuring at different energy resolutions, our QENS results selectively cover the gigahertz to low terahertz frequency range. We have focused on two questions that

Received for publication 10 December 1998 and in final form 11 March 1999.

Address reprint requests to Dr. Thomas Bayerl, Physikalishes Institut EP-5 (Biophysik), Universität Würzburg, Am Hubland, D-97074 Würzburg, Germany. Tel.: 49-931-888-5863; Fax: 49-931-888-5851; E-mail: bayerl@physik.uni-wuerzburg.de.

© 1999 by the Biophysical Society

0006-3495/99/07/331/10 \$2.00

QENS is uniquely suited to tackle: What is the contribution of the cholesterol motion along the bilayer normal to its overall dynamics, and how does its high-frequency dynamics change with temperature? We present possible geometrical models for the motion that may also explain some of the well-established changes of the micromechanical properties of the bilayer caused by this steroid. A particular advantage of the method is that its time scale matches current molecular dynamics (MD) simulations of bilayers. Comparisons between MD and QENS results may improve the molecular interpretation of experimental results and help to refine the force fields and boundary conditions used in the simulations.

MATERIALS AND METHODS

Materials and sample preparation

Deuterated 1,2-dipalmitoyl-d31-glycero-3-phosphocholine-d13 (DPPC-d75) was purchased from Avanti Polar Lipids (Alabaster, AL), and cholesterol was obtained from Fluka (Neu-Ulm, Germany). The DPPC-d75 is perdeuterated, with the exception of the five hydrogen atoms of the glycerol backbone. Highly purified D₂O was purchased from Dechem (Leipzig, Germany). For the solid substrates for multilayer preparation, highly polished, undoped silica wafers of 150- μ m thickness and 5.0-cm diameter were used (Virginia Semiconductors, Fredericksburg, VA). The oriented multilayer samples of DPPC-d75 containing 40 mol% cholesterol and of pure DPPC-d75 were prepared according to procedures described in detail previously (König et al., 1992). Each sample consisted of a stack of 9–10 wafers with \sim 3000 bilayers sandwiched between adjacent wafers, giving a total of 0.4 g lipid per sample. The hydration of the multilayers (20 wt% water) was achieved by equilibrating them against saturated water vapor at a slightly elevated temperature ($T \approx 30^\circ\text{C}$) for a minimum of 30 h before they were stacked. After this the sample was annealed, in saturated vapor, at $T = 95^\circ\text{C}$ for 10 h. Then the samples were transferred to the gas-tight aluminum sample holder for the QENS measurements.

Method

Because QENS is a method rarely used in biophysics, a few basic features of dynamic neutron scattering should be recalled here. In neutron scattering, two scattering cross sections have to be distinguished, the coherent and the incoherent. The former probes the pair-correlation function between different scatterers in a sample and thus provides both structural information and correlated dynamics. Incoherent scattering probes the autocorrelation function of the scattering particles, i.e., the molecular dynamics of the molecules. The possibility of distinguishing the two cross sections makes neutron scattering a unique tool for the determination of dynamical parameters. It is possible to make a deliberate distinction between the two types of scattering simply by choosing a “convenient” scatterer in the sample. For biological applications the most important incoherent scatterer is the hydrogen atom. The deuteron scatters mainly coherently but much more weakly than the incoherent scattering of the proton. Thus (selective) deuteration offers a means of masking (parts of) molecules in incoherent scattering experiments. In our case, the DPPC-d75 was nearly fully deuterated along with the hydration water (D₂O) so that we could selectively observe the incoherent scattering arising from cholesterol. The time scale on which the correlation functions are probed is determined by the energy resolution of the spectrometer used. Hence, by employing various energy resolutions, one can selectively probe different time domains of the correlation function. We used the IN10 backscattering spectrometer and the IN5 time-of-flight spectrometer at the Institut Max von Laue–Paul Langevin (Grenoble, France). The backscattering spectrometer was used in the configuration IN10a (energy analysis by unpolished Si (111) crystals), with

an incident wavelength of 6.271 Å and an energy resolution of 1 μeV . The time-of-flight spectrometer was used at an incident wavelength of 10 Å, giving an energy resolution of 13.67 μeV (Institut Laue-Langevin, 1994). To measure the anisotropy of cholesterol motion and take full advantage of the use of oriented multilayer samples, two orientations of the sample in the neutron beam were measured. At an orientation of 135° between the incident neutron beam and the membrane normal (= normal to the silica wafer), the momentum transfer is directed predominantly perpendicular to the membrane normal (i.e., parallel to the bilayer plane (x-y plane)). In this case the in-plane motion of cholesterol will dominate the incoherent scattering. In contrast, at an orientation of 45° , the momentum transfer is directed predominantly parallel to the membrane normal, and thus the incoherent scattering is dominated by out-of-plane motions of cholesterol along the z-direction (= membrane normal). The scattering geometry is schematically depicted in Fig. 1. Because we were particularly interested in the out-of-plane diffusive motion, we did IN10 measurements at three temperatures for this orientation, $T = 20^\circ\text{C}$, $T = 36^\circ\text{C}$, and $T = 50^\circ\text{C}$, i.e., symmetrically above and below the eutectic temperature ($T = 36^\circ\text{C}$) of the DPPC-d75/cholesterol phase diagram. The in-plane motion (135° orientation) was measured by IN10 at the eutectic temperature ($T = 36^\circ\text{C}$) only. For the higher frequency motions detected by IN5, we measured the in-plane motion at the above three temperatures ($T = 20^\circ\text{C}$, $T = 36^\circ\text{C}$, and $T = 50^\circ\text{C}$) and the out-of-plane motion (45° orientation) at $T = 36^\circ\text{C}$ and $T = 50^\circ\text{C}$. Background subtraction to minimize the contributions of the five glycerol hydrogen atoms per DPPC-d75 molecule to the spectra was achieved by subtracting the corresponding IN10 or IN5 spectra of a pure DPPC-d75 sample measured at $T = 50^\circ\text{C}$. Further standard ILL procedures for background and cell correction as well as normalization of the incoherent scattering to a vanadium standard sample were applied.

Data analysis

The two types of data fitting procedures applied, the single spectrum fitting and the simultaneous fitting procedure, have been described in detail previously (König et al., 1992). The dynamic structure factor $S(\vec{q}, \omega)$ of each motion considered is represented by a sum of Lorentzians (plus an elastic line for motions restricted in space). For a superposition of independent motions contributing to the scattering, the resulting $S(\vec{q}, \omega)$ is the convolution of the corresponding dynamic structure factors for each motion. Fitting the IN10 data to a single Lorentzian (= quasielastic line) gave

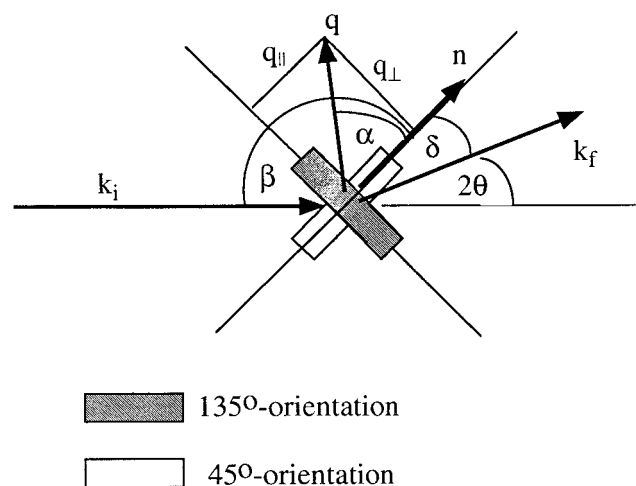


FIGURE 1 Schematic depiction of the scattering geometry used for QENS measurements for oriented membrane stacks. q is the momentum transfer with its components parallel (q_{\parallel}) and perpendicular (\perp) to the membrane normal n . k_i (k_f) is the incoming (final) neutron beam. $\beta \approx 90^\circ - \beta - \theta$ determines the orientation in quasielastic approximation. The scattering vectors, angles, and n are drawn for the case $\beta = 135^\circ$.

a model-independent measure of the translational long-range diffusion coefficient D as listed in Table 1. Note that the term *long-range* refers to any translations over a length of more than 5 Å, the experimental length scale determined by the q -range covered. The second step in data evaluation was to find a model for the motion that is compatible with the observed q -dependencies of the elastic incoherent structure factor (EISF) and line-width. The model function convoluted with the instrument resolution function is then fitted simultaneously to all spectra. The free parameters are the model parameters like long-range diffusion rate (IN10) or jump angle (IN5). For IN10 data, local and long-range diffusions were used simultaneously to describe the data. For the IN5 data analysis, rotational diffusion was considered as the dominant scattering contribution. Three different models were considered (see Appendix), and the number of Lorentzians used in the fit depended on the particulars of the corresponding rotational diffusion model as given in the Appendix. The Debye-Waller factor describes motions that are too fast to be resolved in the time domain used. It was considered in the data analysis analogously to the case described by König et al. (1992).

RESULTS

For a binary mixture of 40 mol% cholesterol in DPPC, QENS measurements were performed for two orientations of the oriented multilayer samples: at 45° and at 135°, corresponding to an energy transfer normal and parallel to the membrane plane. Furthermore, we measured at different energy resolutions (1 μeV (IN10) and 14 μeV (IN5)) corresponding to motional frequencies of the molecules ranging from 0.2 to 50 GHz. The frequency range given here is the range within which one can actually fit a Lorentzian line broadening to our spectra, and not the frequency range accessible to the instruments (IN5 and IN10).

Cholesterol motions along the membrane normal (z direction)

The most striking result at 45° orientation and at the high energy resolution (IN10) is the model-independent evidence for the existence of long-range cholesterol motions in the direction of the membrane normal (z -direction) over distances that are significantly longer than those observed in the plane of the bilayer (x - y plane). This motional anisotropy is clearly seen by comparing the plots of the quasielastic broadening as a function of the squared momentum transfer for both orientations (45° and 135°). This is shown in terms of the half-width at half-maximum (hwhm) in Fig. 2 for the case of $T = 36^\circ\text{C}$, where a significantly stronger

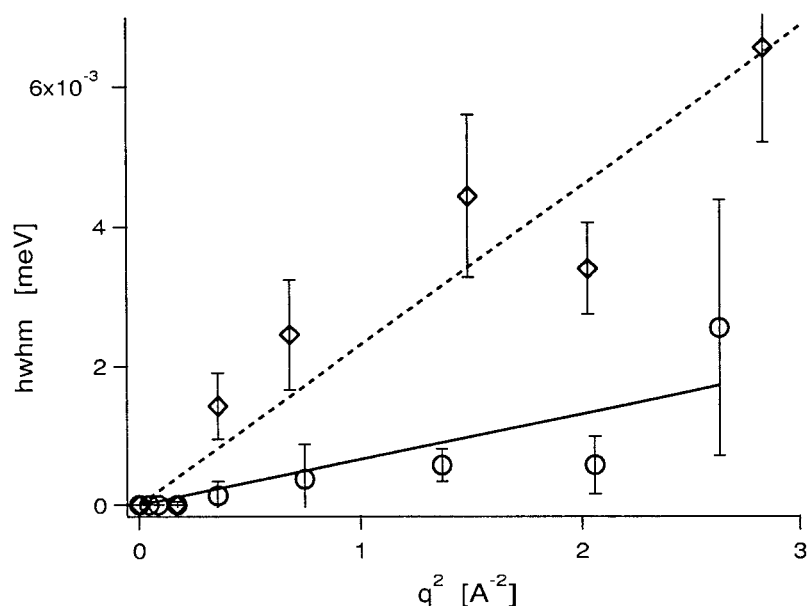
broadening can be observed for the z -direction (orientation 45°). Assuming long-range diffusion as the dominant source of broadening in the IN10 experiments, the corresponding diffusion coefficients D can be estimated from the slope of the straight lines fitted to the data (König et al., 1992) in Fig. 3. Our results for D are listed in Table 1. These results indicate a difference in D of a factor of more than 3 for the two directions (cf. Fig. 2) at a temperature of $T = 36^\circ\text{C}$. In contrast, a plot of the IN5 data in the same way as in Fig. 3 does not give any linear dependence (data not shown). This clearly demonstrates that for the significantly shorter time scale accessible by the IN5 measurement, long-range processes are rendered undetectable, whereas local restricted diffusion is the dominant contribution to the broadening of the signal. We wish to point out that a comparison of the absolute values of D shown in Table 1 with those obtained by NMR or fluorescence methods could be ambiguous for two reasons. First, it should be noted that with a minimum q -value of $\sim 0.2 \text{ \AA}^{-1}$ as used in our measurements, the motion can be observed maximally on a length scale of 5 Å; any restricted motion of cholesterol with amplitudes beyond 5 Å will be seen as long-range diffusion. Second, a detailed data analysis (see below) showed that long-range diffusive motion alone does not describe the IN10 data accurately. There is another, probably local, motional process superimposed within the frequency range of the experiment. Therefore D is not determined solely by pure Fick's diffusion (Bee, 1988) or by hindered diffusion (Egelstaff, 1992). Measurements at even lower energy resolution (e.g., 50 μeV) would be required to separate out even faster and more local motions, as we have demonstrated previously for the case of DPPC motions in a pure DPPC bilayer (König et al., 1992). For a more detailed analysis of cholesterol motion in the normal direction of the bilayer, we assumed that the two overlapping motions are independent, so that the resulting structure factor $S_{\text{sum}}(\vec{q}, \omega)$ is the convolution of the structure factors of the two motions denoted by a and b ; thus $S_{\text{sum}}(\vec{q}, \omega) = S_a(\vec{q}, \omega) \otimes S_b(\vec{q}, \omega)$. In close analogy to our previous QENS work of pure DPPC, we interpret our measured D as a superposition of a long-range diffusion characterized by D_1 and a restricted one-dimensional diffusion described by a local diffusion coefficient D_{1d} along with its spatial extension d_{1d} . To separate the two diffusion coefficients, we used the IN5 data obtained at $T = 36^\circ\text{C}$ for a determination of D_{1d} and d_{1d} . In a second step, we used these results as fixed parameters in the analysis of the IN10 data to obtain D_1 . The results of this procedure are shown in Table 2, and an example of the improved fit in comparison with IN10 raw data is given in Fig. 4.

A second interesting feature of the cholesterol motion in the direction of the bilayer normal is its temperature dependence. We observed an increase of D from $T = 20^\circ\text{C}$ to $T = 36^\circ\text{C}$ by 30%, whereas no further increase in D is observed when T is raised by about the same amount from $T = 36^\circ\text{C}$ to $T = 50^\circ\text{C}$ (cf. Table 1). Table 2 shows that the observed increase in D from $T = 20^\circ\text{C}$ to $T = 36^\circ\text{C}$ can be attributed to both the localized and the long-range process.

TABLE 1 Model-independent long-range diffusion coefficients of cholesterol in DPPC/cholesterol bilayers (lo-phase) in the direction of the bilayer normal (45°) and in the bilayer plane (135°), obtained from the IN10 data fits shown in Fig. 2

Orientation (°)	Temperature (°C)	Long-range diffusion coefficient (m ² /s)
45°	20	$12 \cdot 10^{-12} \pm 13\%$
	36	$17 \cdot 10^{-12} \pm 11\%$
	50	$16 \cdot 10^{-12} \pm 7\%$
135°	36	$5 \cdot 10^{-12} \pm 15\%$

FIGURE 2 Quasielastic line broadening Γ (hwhm) of the IN10 data versus q^2 due to cholesterol motions in the membrane normal direction (orientation = 45° , \diamond , ---) and due to motions in the membrane plane (orientation = 135° , \circ , —) at $T = 36^\circ\text{C}$ in the Dq^2 limit. The lines represent best fits to the data points.



In contrast, between $T = 36^\circ\text{C}$ and $T = 50^\circ\text{C}$ the one-dimensional restricted process increases in D_{1d} while D_1 decreases, resulting in a rather unchanged value of D over this temperature range.

Cholesterol motions within the plane of the bilayer (x-y direction)

For the two energy resolutions used, we analyzed our data in terms of the following motional models: for the high resolution of IN10 (sensitive to motions with longer correlation times), a superposition of long-range and restricted

diffusion as well as two-site jump motions (König et al., 1992) was considered. For the higher frequencies sampled by the IN5 energy resolution, models of either continuous rotation (small-angle jumps) (Dianoux et al., 1975), discrete rotation (large-angle jumps) (Barnes, 1973), or a restricted discrete rotation (cf. second section and Fig. 5 A) were fitted to the data. The latter model describes discrete rotational jumps (one jump = 60° rotational angle), where the jump direction is changed after two successive jumps (i.e., no full rotation). Fig. 6 shows the comparison of the IN5 raw data with the fits according to two of the above-mentioned models (restricted and discrete rotation). The rotational

FIGURE 3 Quasielastic line broadening Γ (hwhm) of the IN10 data versus q^2 due to cholesterol motions in the membrane normal direction (orientation = 45°) at three temperatures ($T = 20^\circ\text{C}$, \circ , ---; $T = 36^\circ\text{C}$, \diamond , —; $T = 50^\circ\text{C}$, \boxtimes , - · -). The lines represent best fits, the slope of which gives the long-range diffusion coefficient D listed in Table 2.

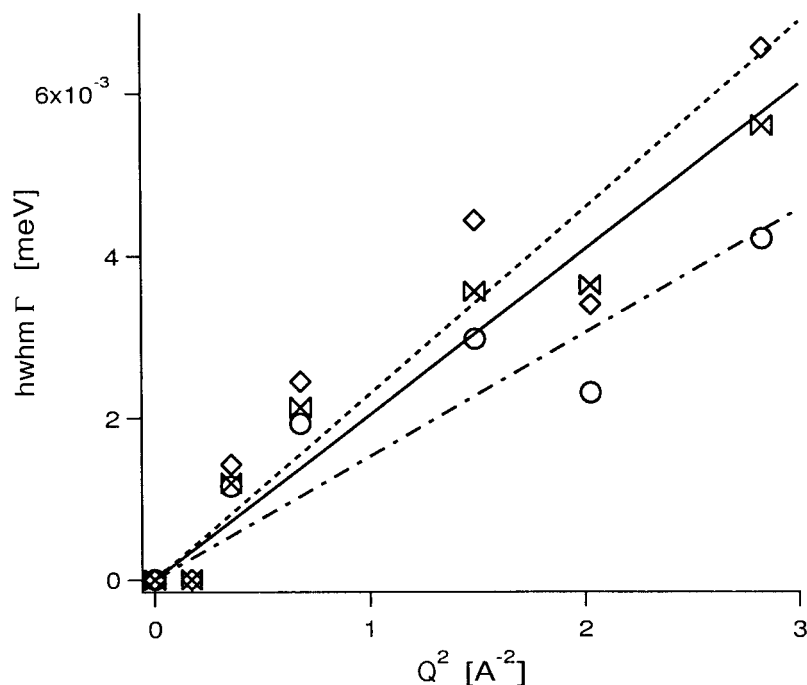


TABLE 2 Results of the model-dependent IN10 and IN5 data fits at three temperatures in the direction of the bilayer normal (45° orientation) and in the bilayer plane (135° orientation)

Orientation (°)	Temperature (°C)	Long-range diffusion coefficient (m ² /s)
45	20	$D_{1d} = 0.4 \times 10^{-12}$ m ² /s
		$d_{1d} = 0.9$ Å
	36	$D_1 = 1.4 \times 10^{-12}$ m ² /s
		$D_{1d} = 30 \times 10^{-12}$ m ² /s
	50	$d_{1d} = 1.9$ Å
		$D_1 = 6.4 \times 10^{-12}$ m ² /s
135	20	$D_{1d} = 34 \times 10^{-12}$ m ² /s
		$d_{1d} = 2.5$ Å
	36	$D_1 = 1.8 \times 10^{-12}$ m ² /s
		$\tau_{rot} = 1.6 \times 10^9$ 1/s
	50	$r_{rot} = 1.9$ Å
		$\tau_{rot} = 2.6 \times 10^9$ 1/s
		$r_{rot} = 2.0$ Å
		$D_{1d} = 2 \times 10^{-12}$ m ² /s
		$d_{1d} = 2.5$ Å
		$\tau_{res} = 2.5 \times 10^9$ 1/s
		$r_{res} = 2.6$ Å

D_{1d} , one-dimensional restricted diffusion; d_{1d} , diffusion length of the one-dimensional restricted diffusion; D_1 , long-range diffusion; τ_{rot} , discrete rotation; r_{rot} , radius of the discrete rotation; τ_{res} , restricted discrete rotation; r_{res} , radius of the restricted discrete rotation.

jump rates and radii extracted from our model fits to the data were in general rather similar for the three models considered. This is illustrated by Fig. 5 B, where the elastic incoherent structure factor (EISF) versus momentum transfer obtained from the IN5 data at $T = 50^\circ\text{C}$ is compared with the corresponding theoretical EISF dependencies for rotational and restricted rotational diffusion. Although the model fits show distinct differences with respect to the minimum EISF values around 1 Å, the experimental error of our IN5 data did not permit us to rule out any particular model. Nevertheless, a global IN5 data analysis of all q -values shows that the two discrete models generally fit the data better than the continuous model. Of the two discrete models, the discrete rotational diffusion with a radius of rotation of 2.0 Å gave the best fits for $T = 20^\circ\text{C}$ and $T = 36^\circ\text{C}$. In contrast, at $T = 50^\circ\text{C}$ the model of restricted rotation proved superior in fitting the data. The results of these discrete rotational model fits as listed in Table 2 indicate a drastic increase in the rotational jump rates by ~70% between $T = 20^\circ\text{C}$ and $T = 36^\circ\text{C}$, whereas no further increase is observed between $T = 36^\circ\text{C}$ and $T = 50^\circ\text{C}$.

To obtain the in-plane long-range diffusion coefficient D_1 from the IN10 data at $T = 36^\circ\text{C}$, we used the IN5 results of the discrete rotation model as fixed parameters in the data fitting while D_1 was considered as a free parameter. The results of this data analysis are listed in Table 2. For $T = 20^\circ\text{C}$ and $T = 50^\circ\text{C}$, only IN5 data were available, so that no information about the temperature dependence of D_1 in the plane of the bilayer can be obtained. Other models employed to fit the IN10 data at $T = 36^\circ\text{C}$ like two-site jumps gave no physically meaningful results.

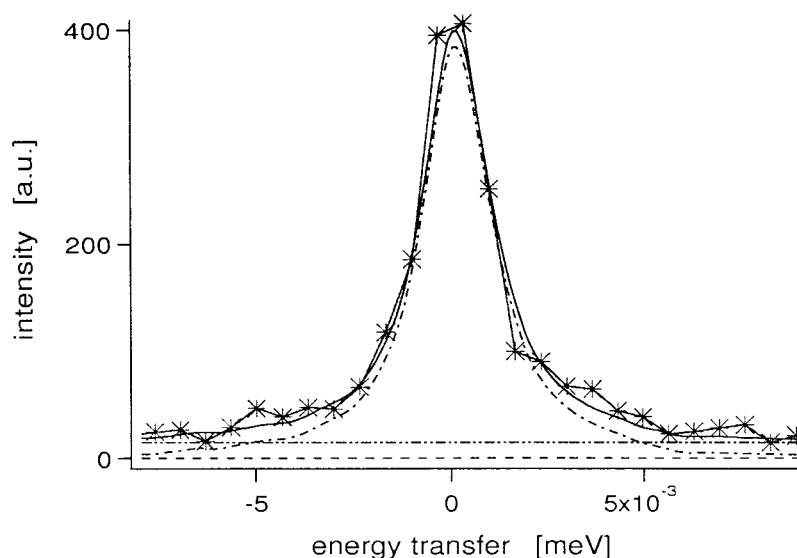
Fig. 7 summarizes the results of our data analysis. At the two lower temperatures, the spatially restricted motion of cholesterol can be considered to fill a cylinder with its axis parallel to the membrane normal. The height of the cylinder increases with temperature and scales with the length over which the restricted diffusion of cholesterol is observed. Its diameter is given by the spatial extension of the diffusive motion in the membrane plane. Beside translations, the molecule performs rotational motions within the cylinder that can be considered as a discrete jump rotation (angle $\alpha = 60^\circ$) at the two lower temperatures and that may become a spatially restricted large angle jump rotation at $T = 50^\circ\text{C}$. Most importantly, these restricted translational and rotational motions are superimposed on a “long-range” diffusion of the whole cylinder parallel to its axis over distances that are significantly larger than the length scale of the experiment (5 Å).

DISCUSSION

The physical properties of the liquid ordered (lo-) phase have been studied previously by a great variety of methods (recently reviewed by McMullen and McElhaney, 1996), and many structural and dynamical features are well established. Nevertheless, no experimental results have been published describing the motion in the direction of the bilayer normal. Incoherent QENS allows such measurements on time and length scales optimally suited for the detection of molecular motions. The above results present the first direct experimental evidence for a motional anisotropy and the existence of a pronounced high-frequency motion of cholesterol in the membrane normal (z) direction. This motion extends over a considerably longer range than that of the lipids in the z -direction. We have demonstrated previously (König et al., 1992) that DPPC alone exhibits a high-frequency, root mean square displacement in the z -direction of 2–3 Å at $T = 50^\circ\text{C}$ (König et al., 1992) under comparable measurement conditions. For cholesterol, however, this displacement is more than 5 Å in z -direction. Moreover, the motional anisotropy of DPPC is opposite that observed here for cholesterol; DPPC shows long-range diffusion in the plane of the bilayer, but only restricted diffusion in the z -direction.

The observed cholesterol long-range diffusion along the bilayer normal is not obvious from purely geometrical considerations. The presence of cholesterol causes local defects in the bilayer that are likely to extend over at least the whole monolayer thickness of the bilayer. The maximum length of the cholesterol molecule (assuming an all-*trans* conformation of its short alkyl chain) is 22 Å (Craven, 1976). For cholesterol in bilayers, it is generally accepted that the (weakly hydrophilic) OH group is oriented toward the lipid headgroup region and that the steroid body penetrates deeply into the hydrophobic tail region of the lipids, down to the bilayer midplane. Assuming now that cholesterol is trapped within an asymmetrical potential in the bilayer with

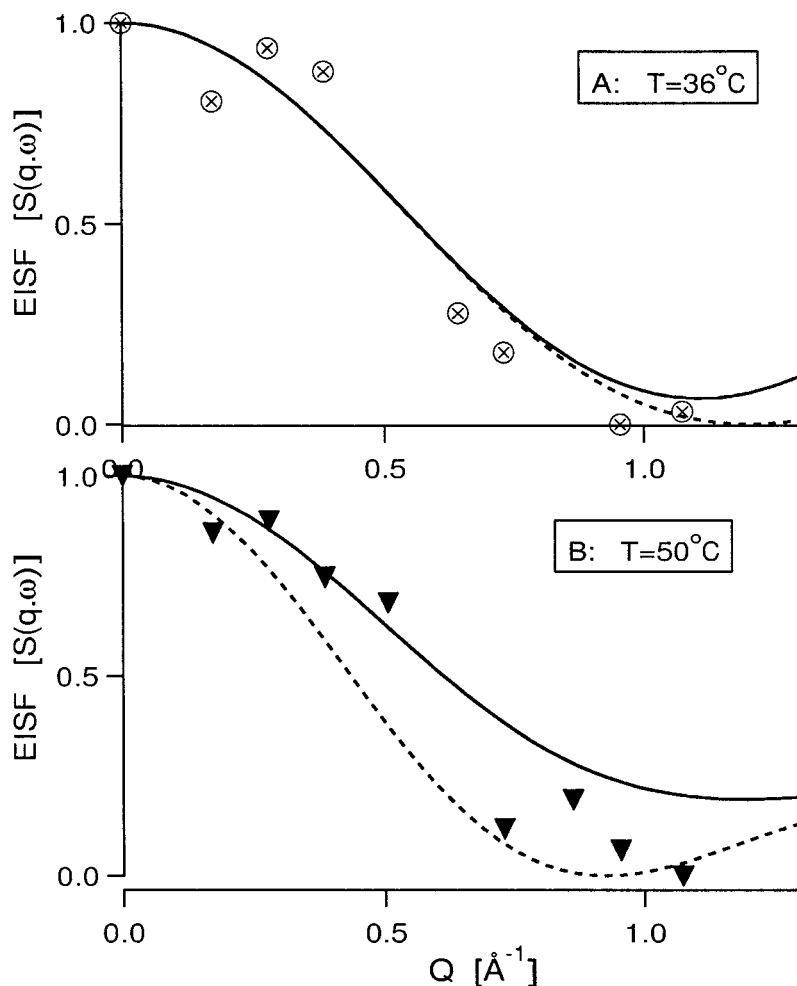
FIGURE 4 Example of the model-dependent fit results of the IN10 data measured at 45° orientation (i.e., momentum transfer parallel to the membrane normal), $T = 36^\circ\text{C}$, for $Q = 0.8 \text{ \AA}^{-1}$ in comparison with the raw data. The experimental data (*), the result of the model calculation (—) and its components, elastic (---), quasielastic (-----), and background (.....), are shown.



a hard wall toward the headgroup region (for the prohibitively high energy required to transfer its hydrophobic parts into this aqueous region), there should be no motional freedom left in the normal direction, because the monolayer

thickness including the headgroup is just 25 \AA at $T = 30^\circ\text{C}$ (Reinl et al., 1992). Even if we assume that cholesterol can penetrate the whole headgroup region of DPPC, the maximum accessible space would be less than 3 \AA per monolayer

FIGURE 5 (A) EISF versus momentum transfer q (IN5 data) at $T = 36^\circ\text{C}$ (\otimes) compared with models of continuous rotational diffusion (---) and of discrete rotational diffusion (—). The radius of rotation is $r = 2.0 \text{ \AA}$ for both models. (B) As in A, but at $T = 50^\circ\text{C}$. Here the data (\blacktriangledown) are compared with the model of continuous rotational diffusion (—) and of restricted rotational diffusion (---); see Appendix A. The radius of rotation is $r = 2.6 \text{ \AA}$ for both models.



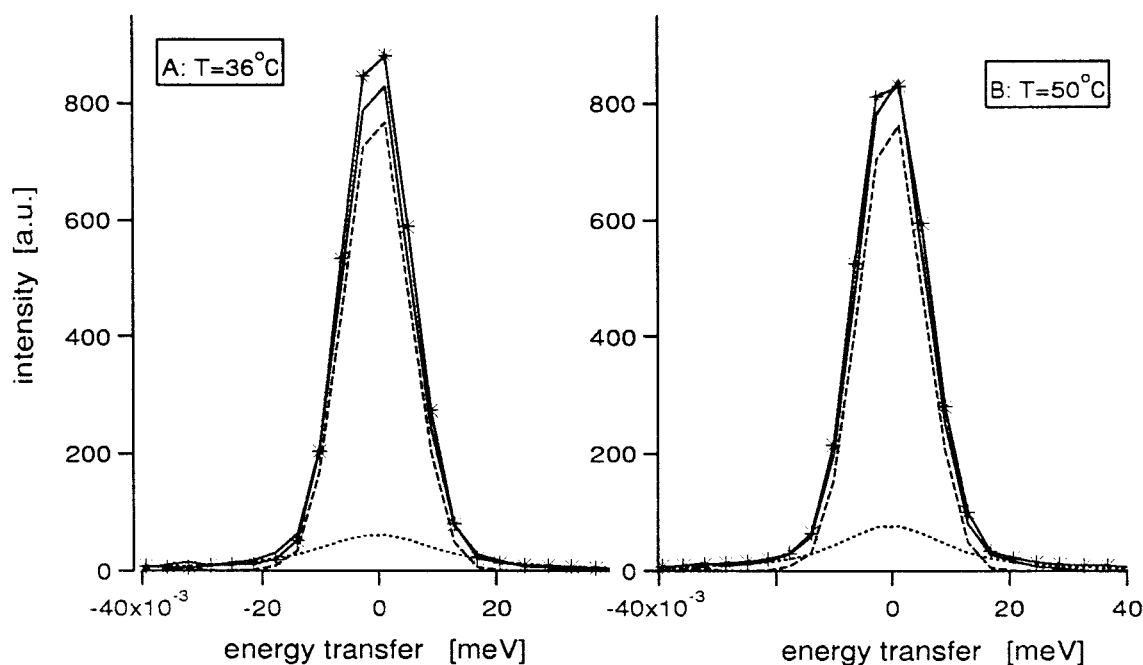


FIGURE 6 (A) Example of the model-dependent fit results (discrete rotation model) of the IN5 data measured at 135° orientation (i.e., momentum transfer in the membrane plane), $T = 36^\circ\text{C}$ for $Q = 0.4 \text{ \AA}^{-1}$ in comparison with the raw data. The experimental data (*), the result of the model calculation (—), and its components, elastic (---), quasielastic (.....), and background (-----), are shown. (B) As in A, but at a higher temperature $T = 50^\circ\text{C}$.

and thus similar to the amplitude of the spatially restricted diffusion observed by IN5 (Table 2).

In contrast to these geometrical considerations, the IN10 results indicate a rather long range of cholesterol diffusion in normal direction over distances of more than 5 \AA . To reconcile geometrical considerations with experimental results, we suggest that cholesterol protrudes dynamically into the opposite monolayer, i.e., that the bilayer midplane is dynamically rough on a molecular scale, at which the steroid bodies are (fluctuating) pillars in a fluid-like environment. Three factors may facilitate this motion:

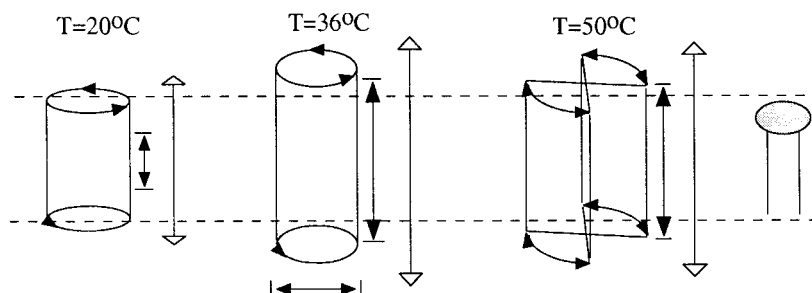
1. The weak hydrophilicity of the cholesterol headgroup.
2. The free volume required for this dynamic protrusion into the opposite monolayer may result from spatial fluctuations of the terminal groups of the lipid tails, owing to the *gauche* conformer formation along the chain. It has been demonstrated previously that such high-frequency displacements of the terminal tail protons over amplitudes of up to 7 \AA exist even in pure

DPPC bilayers (König et al., 1992; Mendelsohn et al., 1989). Davies et al. showed that kinks and single *gauche* conformers dominate the chain disordering in a binary DPPC/cholesterol 2:1 mixture (Davies et al., 1990). Kinks are often considered a driving force for transmembrane movement.

3. The steroid body of cholesterol is rigid, and its short alkyl chain is predominantly in an all-*trans* conformation according to recent molecular dynamics simulations and x-ray studies (Rohrer et al., 1980; Tu et al., 1998).

Hence it may be sufficient that just one palmitoyl chain fluctuates away from the bilayer center to give enough free volume for the partial entry of a cholesterol molecule from the opposite monolayer. The interpretation of our results in terms of a cholesterol fluctuation beyond the confinement of the host lipid monolayer would also explain the presence of both local and long-range diffusion in the z -direction: local motions with amplitudes of $d_{1d} \approx 2 \text{ \AA}$ (Table 2) can be considered as cholesterol motions within the host mono-

FIGURE 7 Schematic depiction of the spatial confinement of cholesterol motions in DPPC bilayers (lo-phase) at three temperatures ($T = 20^\circ\text{C}$, left; $T = 36^\circ\text{C}$, center; $T = 50^\circ\text{C}$, right). Vertical arrows depict the direction of one-dimensional restricted diffusion (full arrows) and of long-range diffusion (open arrows), and curved arrows indicate discrete (left, center) and discrete restricted (right) rotational diffusion. The vertical extension of the cylinders indicates the limits of one-dimensional restricted diffusion.



layer, whereas the long-range contribution reflects those events where the molecule penetrates partially into the opposite monolayer. Among the most striking effects of the presence of cholesterol in the lipid bilayer is the increase of the molecular order parameter (Seelig and Seelig, 1980; Nezil et al., 1992; Vist and Davis, 1990) of the lipid tails and of the bilayer curvature modulus. These effects may be connected with this dynamical process. In particular, it is possible that the fluctuation of cholesterol into the opposite monolayer causes a drastic increase in the frictional drag between the two monolayers, which in turn may increase the bilayer curvature modulus (Needham et al., 1992; Finegold, 1993).

Recent MD simulations of fluid DPPC/cholesterol mixtures suggest a wide distribution of the cholesterol hydroxyl position over a range of ~ 6 Å between the carbonyl and choline positions of the DPPC/cholesterol bilayer (Tu et al., 1998). Although MD and QENS data can, in principle, be compared very directly for their similar time scales, these particular MD results were obtained at a cholesterol concentration of only 12.5 mol%. Thus, they do not reflect exactly the characteristic physical properties of the lo-phase, rendering a detailed comparison ambiguous. Other authors (Gabdoulline et al., 1996) simulated a system closer to ours (DMPC:cholesterol 1:1) but concentrated on the lipid for their data evaluation.

The temperature dependence of the cholesterol motion in the z -direction provides some important clues to the physical properties of the lo-phase. As can be seen from Table 2, both local and long-range diffusion coefficients show a drastic decrease when the temperature is lowered from $T = 36^\circ\text{C}$ to $T = 20^\circ\text{C}$. Simultaneously, a 50% reduction in the amplitude d_{1d} of the local motion is observed. In contrast, an increase in T over a similar temperature range but above the eutectic temperature (from $T = 36^\circ\text{C}$ to $T = 50^\circ\text{C}$) causes only a modest increase in the localized diffusion at a rather unchanged d_{1d} but, concomitantly, a drastic decrease in the long-range diffusion coefficient by a factor of 3. These results appear somewhat contradictory to the established DPPC/cholesterol phase diagram (Vist and Davis, 1990), which considers the lo-phase as homogeneous over the whole temperature range considered in this work. On the other hand, the existence of a phase boundary has been suggested previously on the basis of neutron (Bayerl and Sackmann, 1993) and NMR (Reinl et al., 1992) data. From the dynamical QENS point of view, the drastic changes of the overall cholesterol dynamics between $T = 20^\circ\text{C}$ and $T = 50^\circ\text{C}$ strongly suggest a transition between different dynamical states that might be connected with the existence of a hidden phase boundary.

It is interesting to compare our temperature dependence of high-frequency cholesterol motion with that obtained for the lipid component (DPPC) in the lo-phase by other spectroscopic methods. Deuterium NMR and Fourier transform infrared (FTIR) spectroscopies of oriented DPPC/cholesterol multilayers have provided evidence for a largely unchanged molecular order parameter of the methylene groups

along the palmitoyl chains in the same temperature range (Reinl et al., 1992). However, in the same publication, FTIR also showed a significant increase in end-*gauche* states of their methyl groups between $T = 36^\circ\text{C}$ and $T = 41^\circ\text{C}$. Based on an analysis of the terminal methyl quadrupolar splittings, it was suggested that cholesterol is driven away from the bilayer center, toward the aqueous interface with increasing temperature. Therefore, these FTIR results seem to support our findings regarding the change of the vertical dynamics of cholesterol with temperature.

Taking the above NMR results into account, we interpret our QENS results in terms of a change in the dynamical state of cholesterol with temperature as follows:

1. At $T = 20^\circ\text{C}$, cholesterol vertical motion is largely restricted to the confinement of the host monolayer due to the high order of the lipid tails, including their terminal methyl groups.
2. At $T = 36^\circ\text{C}$, an increase in the number of end-*gauche* conformers of the lipid tails allows the cholesterol to fluctuate into the opposite monolayer.
3. At $T = 50^\circ\text{C}$, the decrease in bilayer thickness by at least 4 Å, due to an increased number of *gauche* conformers along the palmitoyl chains, forces the cholesterol off the bilayer center toward the interface. This lowers the long-range contribution D_1 (cf. Table 2), because a penetration into the opposite monolayer becomes less likely and a diffusion into the aqueous bulk is unfavorable for energetic reasons.

Our results obtained for cholesterol motions in the bilayer plane (x - y plane) agree well with conclusions drawn from deuterium NMR relaxation experiments using selectively deuterated cholesterol in DPPC bilayers. In agreement with our data analysis, the NMR measurements exclude a continuous rotation of cholesterol, i.e., the cholesterol molecule's residence time on a site cannot be neglected in comparison to the time required for a jump to the next site. Regarding the distinction between discrete and restricted discrete rotation (jumps between a fixed number of sites on a circle), the NMR comes to somewhat contradictory results. Whereas Bonmatin et al. (1990) suggested a model of discrete rotation with a jump frequency of 30 MHz, a restricted rotational diffusion with a frequency of 1 GHz was postulated in the work of Weisz (Weisz et al., 1992). Even though all three models used are possible as judged from the model-independent analysis, global fits to the data suggest discrete models.

The temperature dependence of the IN5 in-plane results can be interpreted in terms of a significant reduction of the rotational motion upon cooling the system from $T = 36^\circ\text{C}$ to $T = 20^\circ\text{C}$ (Table 2). This process seems to be coupled with a change of the lipid rotation, as suggested previously from lineshape changes of deuterium NMR spectra of chain-deuterated DPPC in the lo-phase (Vist and Davis, 1990). It is remarkable that no significant changes in cholesterol rotation were observed for the temperature range $T = 36^\circ\text{C}$ to $T = 50^\circ\text{C}$. A possible explanation could be the

dominance of a rattling motion of cholesterol at elevated temperatures, which would leave its rotational jump rates essentially unchanged. A similar feature was observed previously for the lipid motion in pure DPPC bilayers (Koenig and Sackmann, 1996).

CONCLUSIONS

We have shown that cholesterol motion in DPPC bilayers is highly anisotropic in the high-frequency regime (~ 1 GHz) with respect to the two orientations studied and exhibits a surprisingly large extension of diffusive motions parallel to the membrane normal. The latter exceeds the geometrical limits of the host DPPC monolayer leaflet at elevated temperatures. The formation of hydrogen bonds between cholesterol and DPPC headgroups seems unlikely at higher temperatures but might become important at the lower temperature limit of our experiments ($T = 20^\circ\text{C}$). At this temperature, a clustering of cholesterol into more immobile aggregates could be possible, as proposed by Knoll et al. (1985), but our results do not allow us to draw any conclusions in this direction. Nevertheless, we have clearly shown that the lo-phase is not homogeneous from the dynamical point of view in the lower temperature range. This dynamical phase boundary may be connected with the above-mentioned confinement of the cholesterol motion vertical to the host monolayer observed at low temperature ($T = 20^\circ\text{C}$).

APPENDIX: CALCULATION OF RESTRICTED, DISCRETE ROTATION

Different models of rotation and other in-plane motions have been suggested for cholesterol, such as discrete rotation (Barnes, 1973), rotational diffusion (Dianoux et al., 1975), diffusion inside a circle (Dianoux et al., 1982), and two-site jump models (Bee, 1988). However, none of them consider the possibility that the rotation is spatially restricted because of the presence of obstacles formed by adjacent molecules like the lipid tails under tight packing conditions. In the following, we will present a model for such a partial rotational diffusion that considers a discrete rotation (Bonmatin et al., 1990) constrained by the presence of obstacles that prevent a full rotation. Fig. 8 depicts schematically a top view of this

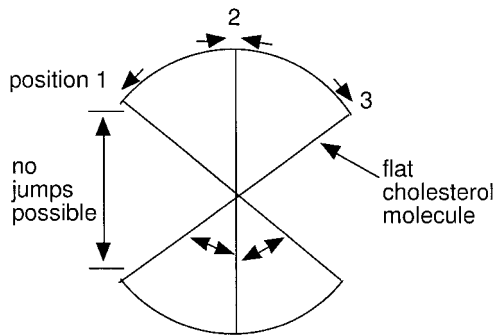


FIGURE 8 Schematic depiction (top view) of our model of a restricted discrete rotation of cholesterol within a lipid bilayer. The direction of rotation is reversed after two consecutive jumps in the same direction over a 60° angle.

model. The calculation of the scattering law is analogous to the procedure suggested by Barnes (1973). Starting from the intermediate scattering function,

$$I_{\text{inc}}(\vec{q}, t) = \langle e^{i\vec{q}(\vec{r}(0) - \vec{r}(t))} \rangle$$

$$= \frac{1}{N} \sum_{j=1}^N \mathcal{P}_{jN}(t) e^{i\vec{q}(\vec{r}_N - \vec{r}_j)}, \quad (\text{A1})$$

where \mathcal{P} is the probability matrix that a jump will occur, N is the number of lattice sites, \vec{q} is the momentum transfer, \vec{r} is the space, and t is the time dependence of the motion. The brackets $\langle \rangle$ denote the thermal average. To obtain this result (Eq. A1), we make use of the fact that all starting positions have equal probabilities. Assuming uncorrelated jumps, the probability matrix and its eigensystem (eigenvector E , eigenvalue λ) are

$$\mathcal{P}^{(1)} = \begin{pmatrix} 1-p & p & 0 \\ p & 2-p & p \\ 0 & 1-p & p \end{pmatrix},$$

$$\lambda_1 = 1, \quad \lambda_2 = 1 - 3p, \quad \lambda_3 = 1 - p,$$

$$\vec{E}^{(1)} = \left(\frac{1}{\sqrt{3}}, \frac{1}{\sqrt{3}}, \frac{1}{\sqrt{3}} \right), \quad \vec{E}^{(2)} = \left(\frac{1}{\sqrt{6}}, \frac{-2}{\sqrt{6}}, \frac{1}{\sqrt{6}} \right),$$

$$\vec{E}^{(3)} = \left(\frac{-1}{\sqrt{2}}, 0, \frac{1}{\sqrt{2}} \right). \quad (\text{A2})$$

Following the procedure of Barnes et al. (Barnes, 1973), we transform the steps in a random walk problem to a time-dependent function by defining a rate constant K such that $p = K \Delta t$, where Δt is the time needed for one step. Let $n = t/\Delta t$, and allow Δt to approach 0. We then Fourier transform the result from the time to the energy domain and average over all in-plane positions. This gives the dynamic incoherent structure factor $S(\vec{q}, \omega)$, which is the space and time Fourier transform of the autocorrelation function (van Hove, 1954) and can be written as an elastic line (δ -function) and a sum of Lorentzian broadening lines L :

$$S(\vec{q}, \omega) = A_0(\vec{q})\delta(\omega) + A_1(\vec{q})L_1(\Gamma_1, \vec{q}) + \dots$$

$$= 1 * \delta(\omega) + \frac{4}{3} \cos(\vec{q}_{\parallel} \vec{r}_a) \cos(\theta) J_0(\vec{q}_{\perp} \vec{r}_a \sin(\theta))$$

$$* L_1(\Gamma_1 = -3p, \vec{q})$$

$$+ \frac{2}{3} \cos(\vec{q}_{\parallel} \vec{r}_b) \cos(\theta) J_0(\vec{q}_{\perp} \vec{r}_b \sin(\theta)) * L_2(\Gamma_2 = -p, \vec{q}), \quad (\text{A3})$$

where ω is the energy transfer, and θ is the angle between the membrane normal \vec{n} and the direction of the jump \vec{r} (assumed to be $\theta = 90^\circ$ in our model). J_0 is the cylindrical Bessel function of 0th order. $L_n(\Gamma_n, \vec{q})$ is the n th quasielastic broadening of Lorentzian lineshape of the width Γ_n (half-width at half-maximum, hwhm). The A_n are the amplitudes of the Lorentzian broadening L_n , $\sum_n A_n = 1$. \vec{q}_{\parallel} and \vec{q}_{\perp} denote the q -vectors parallel and perpendicular to the membrane normal. Further assuming a jump angle of $\alpha = 60^\circ$, we obtain

$$\vec{r}_a = \vec{r}, \quad \vec{r}_b = \sqrt{3}\vec{r}. \quad (\text{A4})$$

This model gives theoretical EISF versus q and hwhm versus q dependencies, which were compared to those obtained experimentally. The results are shown for the IN5 data in Fig. 5.

REFERENCES

- Almeida, P. F. F., W. Vaz, and T. Thompson. 1992. Lateral diffusion in the liquid phases of dimyristoylphosphatidylcholine/cholesterol lipid bilayers: a free volume analysis. *Biochemistry*. 31:6739–6747.
- Barnes, J. D. 1973. Inelastic neutron scattering study of the rotator phase transition in *n*-nonadecane. *J. Chem. Phys.* 53:5193–5201.
- Bayerl, T. M., and E. Sackmann. 1993. Neutron scattering as a tool to probe the effect of cholesterol on phase separation, structure formation, and lipid/protein interaction in artificial membranes. In *Cholesterol and Membrane Models*. CRC Press, Boca Raton, FL. 13–43.
- Bee, M. 1988. Quasielastic Neutron Scattering: Principles and Applications in Solid State Chemistry, Biology, and Materials Science. Adam Hilger, Bristol.
- Bonmatin, J.-M., I. Smith, H. Jarrell, and D. Siminovitch. 1990. Use of a comprehensive approach to molecular dynamics in ordered lipid systems: cholesterol reorientation in orientated lipid bilayers. *J. Am. Chem. Soc.* 112:1697–1704.
- Brown, M. 1990. Anisotropic nuclear spin relaxation of cholesterol in phospholipid bilayers. *Mol. Phys.* 71:903–908.
- Craven, B. M. 1976. Crystal structure of cholesterol monohydrate. *Nature*. 260:727–729.
- Davies, M. A., H. Schuster, J. Brauner, and R. Mendelsohn. 1990. Effects of cholesterol on conformational disorder in dipalmitoylphosphatidylcholine bilayers. A quantitative IR study of the depth dependence. *Biochemistry*. 29:4368–4373.
- Dianoux, A. J., F. Pineri, and M. Volino. 1982. Neutron incoherent scattering law for restricted diffusion inside a volume with an anisotropic shape. Application to the problem of water absorbed in nafion membranes. *Mol. Phys.* 46:129–137.
- Dianoux, A. J., F. Volino, and H. Hervet. 1975. Incoherent scattering law for neutron quasi-elastic scattering in liquid crystals. *Mol. Phys.* 30:1181–1194.
- Egelstaff, P. 1992. An Introduction to the Liquid State. Oxford Science Publication, Oxford.
- Finegold, L., editor. 1993. Cholesterol and Membrane Models. CRC Press, Boca Raton, FL.
- Gabdoulline, R. R., G. Vanderkooi, and C. Zheng. 1996. Comparison of the structures of dimyristoylphosphatidylcholine in the presence and absence of cholesterol by molecular dynamics simulations. *J. Phys. Chem.* 100:15942–15946.
- Huang, T. H., C. Lee, S. K. Das Gupta, A. Blume, and R. Griffin. 1993. A C-13 and H-2 nuclear magnetic resonance study of phosphatidylcholine/cholesterol interactions—characterization of liquid-gel phases. *Biochemistry*. 32:13277–13287.
- Institut Laue-Langevin. 1994. Guide to the Neutron Research Facilities at the ILL. Institut Laue-Langevin, Grenoble, France.
- Ipsen, J. H., G. Karlström, O. Mouritsen, H. Wennerström, and M. Zuckermann. 1987. Phase equilibria in the phosphatidylcholine-cholesterol system. *Biochem. Biophys. Acta*. 905:162–172.
- Ipsen, J. H., O. Mouritsen, and M. Bloom. 1990. Relationship between lipid membrane area, hydrophobic thickness and acyl-chain orientational order. The effect of cholesterol. *Biophys. J.* 57:405–412.
- Ipsen, J. H., O. Mouritsen, and M. Zuckermann. 1989. Theory of thermal anomalies in the specific heat of lipid bilayers containing cholesterol. *Biophys. J.* 56:661–667.
- Knoll, W., G. Schmidt, and K. Ibel. 1985. Incoherent scattering correction for forward scattering of neutrons by aqueous buffers, temperature dependence and influence of absorbing salts. *J. Appl. Crystallogr.* 18:517–524.
- König, S., W. Pfeiffer, T. Bayerl, D. Richter, and E. Sackmann. 1992. Molecular dynamics of lipid bilayers studied by incoherent quasi-elastic neutron scattering. *J. Phys. France*. 2:1589–1615.
- König, S., and E. Sackmann. 1996. Molecular and collective dynamics of lipid bilayers. *Curr. Opin. Coll. Int. Sci.* 1:78–82.
- McMullen, T. P. W., and R. McElhaney. 1996. Physical studies of cholesterol-phospholipid interactions. *Curr. Opin. Colloid Interface Sci.* 1:83–90.
- Mendelsohn, R., M. Davies, J. Brauner, H. Schuster, and R. Dluhy. 1989. Quantitative determination of conformational disorder in the acyl chains of phospholipid bilayers by infrared spectroscopy. *Biochemistry*. 28:8934–8939.
- Needham, D., T. McIntosh, and D. Lasic. 1992. Repulsive interactions and mechanical stability of polymer-grafted lipid membranes. *Biophys. Biochim. Acta*. 1108:40–48.
- Nezil, F. A., S. Bayerl, and M. Bloom. 1992. Temperature-reversible eruptions of vesicles in model membranes studied by NMR. *Biophys. J.* 61:1413–1426.
- Reinl, H., T. Brumm, and T. Bayerl. 1992. Changes of the physical properties of the liquid/ordered phase with temperature in binary mixtures of DPPC with cholesterol. A ²H-NMR, FT-IR, DSC and neutron scattering study. *Biophys. J.* 61:1025–1035.
- Rohrer, A. J., W. Richards, J. Griffin, and C. Weeks. 1980. Conformational analysis of sterols: comparison of x-ray crystallographic observations with data from other sources. *Lipids*. 15:783–792.
- Seelig, J., and A. Seelig. 1980. Lipid conformation in model membranes and biological membranes. *Q. Rev. Biophys.* 13:19–61.
- Siminovitch, D. J., M. Ruocco, A. Makriyannis, and R. Griffin. 1987. The effect of cholesterol on lipid dynamics and packing in diether phosphatidylcholine bilayers. X-ray diffraction and ²H-NMR study. *Biochim. Biophys. Acta*. 901:191–200.
- Siminovitch, D. J., M. Ruocco, E. Olejniczak, S. dasGupta, and R. Griffin. 1988. Anisotropic ²H-nuclear magnetic resonance spin-lattice relaxation in cerebroside- and phospholipid-cholesterol bilayer membranes. *Biophys. J.* 54:373–381.
- Tobias, D. J., K. Tu, and M. Klein. 1997. Atomic-scale molecular dynamics simulations of lipid membranes. *Curr. Opin. Colloid Interface Sci.* 2:15–26.
- Tu, K., M. Klein, and D. Tobias. 1998. Constant pressure molecular dynamics investigation of cholesterol effects in a DPPC bilayer. *Biophys. J.* 75:2147–2156.
- van Hove, L. 1954. Correlations in space and time and Born approximation scattering in systems of interacting particles. *Phys. Rev.* 95:249–262.
- Vist, M. R., and J. Davis. 1990. Phase equilibria of cholesterol/DPPC mixtures: ²H-NMR and DSC. *Biochemistry*. 29:451–464.
- Weisz, K., G. Grobner, C. Mayer, J. Stohrer, and G. Kothe. 1992. Deuteron nuclear magnetic resonance study of the dynamic organization of phospholipid cholesterol bilayer membranes—molecular properties and viscoelastic behavior. *Biochemistry*. 31:1100–1112.